Available online at www.sciencedirect.com
SCIENCE DIRECT®
ELSEVIER
International Journal of Solids and Structures 43 (2006) 3905–3919
INTERNATIONAL JOURNAL OF SOLIDS and STRUCTURES
www.elsevier.com/locate/ijsolstr

Dynamic buckling of cylindrical shells subject to an axial impact in a symplectic system

Xinsheng Xu [a,*], Yuan Ma [a], C.W. Lim [b], Hongjie Chu [a]

[a] *State Key Laboratory of Structure Analysis of Industrial Equipment and Department of Engineering Mechanics, Dalian University of Technology, Dalian 116024, PR China*
[b] *Department of Building and Construction, City University of Hong Kong, Hong Kong*

Received 3 March 2005
Available online 12 April 2005

Abstract

This paper discusses the dynamic pre-buckling of finite cylindrical shells in the propagation and reflection of axial stress waves. By introducing the Hamiltonian system into dynamic buckling of structures, the problem can be described mathematically in a symplectic space. The solutions of Hamiltonian dual equations shown in canonical variables are obtained. The problem is reduced to the determination of eigenvalues and eigensolutions, with the former indicating critical buckling loads and the latter buckling modes. Numerical example presented shows phenomena of axisymmetric and non-axisymmetric dynamic buckling subject to impacts of axial load.

Keywords: Dynamic buckling; Duality system; Symplectic space; Shell; Stress wave

1. Introduction

There has been intensive attention on dynamic buckling of structures as compared to static buckling problems because the former has significant engineering characteristics as well as important design implications. Dynamics buckling is local and it involves an extension process. The local phenomena have relations with propagation of stress waves proven by experiments. Therefore, it is necessary and far-reaching to discuss dynamic buckling of structures with respect to propagation and reflection of waves.

* Corresponding author. Tel.: +86 41184708393; fax: +86 41184708393.
E-mail addresses: xsxu@dlut.edu.cn (X. Xu), mayuan945@163.com (Y. Ma), bccwlim@cityu.edu.hk (C.W. Lim), forefancy.student@sina.com (H. Chu).

0020-7683/$ - see front matter
doi:10.1016/j.ijsolstr.2005.03.005

Nomenclature

E	Young's modulus
μ	Poisson's ratio
ρ	material density
h, r, l	thickness, middle surface radius and length of cylindrical shell, respectively
(r, θ, x)	circular cylindrical coordinate
u	x-axial, centroidal axial, displacement of a shell
w	lateral displacement
v	circumferential displacement
D, K	$D = Eh^3/[12(1-\mu^2)]$ and $K = Eh/(1-\mu^2)$, the shell felxural rigidity and stiffness
$\varepsilon_i, \varepsilon_{ij}$	membrane strains and shear strains in the neutral surface
κ_i, τ	bending and torsional strains in the neutral surface
N_i, N_{ij}	internal stresses and shear stresses
M_i, M_{ij}	bending and torsional moments
c	$c = [E/\rho(1-\mu^2)]^{1/2}$, wave speed
N	axial compressive load
L	Lagrange function
H	Hamiltonian function
$\mathbf{q}, \mathbf{p}$	mutually dual vectors
$\mathbf{H}$	Hamiltonian operator matrix

For more than 40 years, dynamic buckling of cylindrical shells subject to axial impact has been of intensive study. Coppa (1960) discovered in an experiment that the mode of dynamic buckling is similar to that of static buckling. Through experiments, Wang et al. (1983) reported that axisymmetric and non-axisymmetric buckling modes depend upon the axial impact velocity and the thickness of cylindrical shells. They put forward the first and second critical velocities in allusion to two modes upwards in the middle thickness shell. Ma et al. (2003) further discussed the second critical velocities. Besides, the effect of stress wave was noticed in experiments (Chen et al., 1992) which explored the connection between axial stress waves and buckling phenomena. Theoretical methods and numerical results in agreement with physical phenomenon and experiments have been developed. Xu et al. (1995, 1997a) discussed dynamics of axisymmetric and non-axisymmetric buckling, respectively, in which the propagation of axial stress wave was considered using the method of modal functions. With the aid of the modal method, Jamal et al. (2004), Abdullah et al. (2003) and Sofiyev and Aksogan (2004) recently investigated some buckling problems of cylindrical shells. However, the method requires expansion of modal functions to solve partial differentiations, in which the space of solutions is not complete. With respect to numerical methods, a number of researchers discussed buckling of cylindrical shells by using finite element method Choong and Ramm (1998), mixed finite elements (Uchiyama and Yamada, 2003), p-element method (Lim and Ma, 2003; Lim et al., 2003), the Ritz method (Tian et al., 1999) and asymptotic-numerical method (Fettahli and Steele, 1974; Tovstik and Smirnov, 2001; Boutyour et al., 2004). Karagiozova and Jones (2001, 2002) considered the influence of stress waves by employing the finite element method and analyzed dynamic progressive buckling from in the viewpoint of the authors wave propagation resulting from an axial impact. Karagiozova and Alves (2004a,b) studied buckling problem via the combination of theoretical analysis, experiment, numerical analysis and observation. These works revealed distinctly some phenomenon and behaviors of bucklings of cylindrical shell. In various investigations, specific attention has been paid to the fact that the buckling load of thin cylindrical shell under axial compression depends significantly on the initial imperfection of the specimen. Because of

imperfection sensitivity, modes and extended process of post-buckling of shells cannot be ensured. For this problem, quantitative analyses have been published by scholars, for example Florence and Goodier (1968), Arbocz and Hol (1991), Hambly and Calladine (1996), Jamal et al. (1999) and Lancaster et al. (2000). The supposition of initial imperfections should be appropriate or else results cannot be convincing. In the author's viewpoint, it should be reasonable that pre-buckling modes are considered as initial imperfections of post-buckling problems.

The methods mentioned above belong to the Lagrange formulation which is difficult for solving higher order partial differentiations. By introducing Hamiltonian formulation into theory of elasticity, the method of separation of variables has been generalized. Zhong (2004) investigated the plane problem of isotropic elasticity with the aid of Hamiltonian system. Steele and Kim (1992) established a modified mixed variational principle and the state-vector equation, i.e. the Hamiltonian canonical equation, for elastic bodies and shells with spatial variables as the independent variables. In the Hamiltonian system, there exists an adjoint symplectic ortho-normalization relationship with the corresponding expansion theorem among the eigenfunction-vectors in elasticity (Zhong, 2004; Xu et al., 1997b). From this symplectic system, complete solutions can be obtained.

In this paper, the Hamiltonian formulation for dynamic buckling of shells is investigated. In the propagation of longitudinal waves resulted from axial impact loads, the fundamental equations or the dual equations and the corresponding boundary conditions are obtained. In the symplectic space, the critical buckling loads and modes are described by a direct method with the aid of a complete space of solutions.

2. The fundamental problem

Consider an elastic cylindrical shell with thickness h, middle surface radius r, length l, Young's modulus E and Poisson's ratio μ. The shell is subjected to an axial impact load at the end ($x = 0$). A circular cylindrical coordinate (r, θ, x) is adopted such that the x-axis is along the centroidal axis and (w, v, u) are the corresponding displacements. The constitutive relations are expressed as

$$\begin{cases} N_x = K(\varepsilon_x + \mu\varepsilon_\theta) \\ N_\theta = K(\varepsilon_\theta + \mu\varepsilon_x) \\ N_{x\theta} = K(1-\mu)\varepsilon_{x\theta}/2 \\ M_x = D(\kappa_x + \mu\kappa_\theta) \\ M_\theta = D(\kappa_\theta + \mu\kappa_x) \\ M_{x\theta} = D(1-\mu)\tau \end{cases} \tag{1}$$

where $D = Eh^3/[12(1-\mu^2)]$ and $K = Eh/(1-\mu^2)$. The membrane strain components and curvature components in the neutral surface are

$$\begin{cases} \varepsilon_x = \dfrac{\partial u}{\partial x} \\ \varepsilon_\theta = \frac{1}{r}\dfrac{\partial v}{\partial \theta} - \dfrac{w}{r} \\ \varepsilon_{x\theta} = \dfrac{1}{r}\dfrac{\partial u}{\partial \theta} + \dfrac{\partial v}{\partial x} \end{cases} \quad \begin{cases} \kappa_x = -\dfrac{\partial^2 w}{\partial x^2} \\ \kappa_\theta = -\dfrac{1}{r^2}\dfrac{\partial^2 w}{\partial \theta^2} \\ \tau = -\dfrac{1}{r}\dfrac{\partial^2 w}{\partial x \partial \theta} \end{cases} \tag{2}$$

The extension potential energy density, bending potential energy density, work of external load and kinetic energy of the shell subjected to an axial impact load are denoted by Π_ε, Π_κ, Π_w and Π_t, respectively.

The Lagrange function can be shown as

$$\begin{aligned}\Pi &= \Pi_\varepsilon + \Pi_\kappa + \Pi_w - \Pi_t \\ &= \frac{1}{2}K\left(\varepsilon_x^2 + \varepsilon_\theta^2 + 2\mu\varepsilon_x\varepsilon_\theta + \frac{1-\mu}{2}\varepsilon_{x\theta}^2\right) + \frac{1}{2}D(\kappa_x^2 + \kappa_\theta^2 + 2\mu\kappa_x\kappa_\theta + 2(1-\mu)\tau^2) - \frac{N}{2}\psi_x^2 - \frac{1}{2}\rho h\left(\frac{\partial u}{\partial t}\right)^2\end{aligned} \tag{3}$$

where $\psi_x = -\partial w/\partial x$ is the bending angle, ρ the material density and N an axial compressive load. Consider internal forces uniformity along the circumferential direction, the Lagrange function becomes

$$\begin{aligned}L = {} & \frac{K}{2}\left(\frac{\partial u}{\partial x}\right)^2 - \frac{\rho h}{2}\left(\frac{\partial u}{\partial t}\right)^2 + \frac{K}{2r^2}w^2 \\ & + \frac{D}{2}\left\{\left(\frac{\partial^2 w}{\partial x^2}\right)^2 + \frac{1}{r^4}\left(\frac{\partial^2 w}{\partial\theta^2}\right)^2 + \frac{2}{r^2}\frac{\partial^2 w}{\partial x^2}\frac{\partial^2 w}{\partial\theta^2} - \frac{(1-\mu)}{r^2}\left[\frac{\partial^2 w}{\partial x^2}\frac{\partial^2 w}{\partial\theta^2} - \left(\frac{\partial^2 w}{\partial x\partial\theta}\right)^2\right]\right\} - \frac{N}{2}\left(\frac{\partial w}{\partial x}\right)^2\end{aligned} \tag{4}$$

Employing the principle of minimum potential energy, the governing equations expressed in terms of displacements can be obtained. The displacement method belongs to the Lagrange formulation or it is a Lagrange system.

3. Propagation and reflection of longitudinal stress wave

It is noticed that the longitudinal wave equation can be obtained from Eq. (4) via a variational approach. The process results in decoupling of other equations. The equation is

$$\frac{\partial^2 u}{\partial t^2} - c^2\frac{\partial^2 u}{\partial x^2} = 0 \tag{5}$$

where the wave speed is $c = [E/\rho(1-\mu^2)]^{1/2}$. The axial force can be confirmed by wave propagation base on wave equation and the end conditions, with an impact at $x = 0$ and with no impact at $x = l$. The boundary condition is about longitudinal displacement u. It implies a temporal function of force, or $N = N(x, t)$. In this case, we may assume a stepped axial impact load $N_x(0, t) = -NH(t)$, where N is a constant and $H(t)$ is a step function: $H(t) = 1$ if $t \geqslant 0$ and $H(t) = 0$ if $t < 0$. When an impact at the end of shell takes place, the longitudinal stress wave begins to propagate from the end and the elastic wave front is $x_e = ct$. After the wave arrives at the other end, the longitudinal wave reflects. Here, we assume the reflection end is a clamped support, or $u(l, t) = 0$, and only the first reflection ($t < 2l/c$) is considered. For an ideal, perfect shell the axial internal force for propagation and reflection of wave can be expressed as (Xu et al., 1997a)

$$N_x = \begin{cases} -N & 0 \leqslant x \leqslant x_e, t \leqslant l/c \\ 0 & x_e < x \leqslant l, t \leqslant l/c \\ -N & 0 \leqslant x < x_r, t > l/c \\ -2N & x_r \leqslant x \leqslant l, t > l/c \end{cases} \tag{6}$$

where the reflection of wave front is $x_r = 2l - ct$.

4. Hamiltonian system and the adjoint symplectic ortho-normalization

Consider an elastic shell with radius r as the character length measured from the shell middle surface. We adopt the dimensionless parameters $X = x/r$, $W = w/r$, $L = l/r$, $T = tc/r$ and $\gamma = (r/h)^2/12$, $N_{cr} = Nr^2/D$. Let an over-dot denotes differentiation with respect to X, namely $(\cdot) = (\partial/\partial X)(\ )$ in which the X-coordinate can

be taken in analogy to the time coordinate, and $(\ )' = (\partial/\partial\theta)(\ ) \equiv \partial_\theta(\ )$. The dimensionless Lagrange function correlated with radial displacement W can be simplified as

$$L(W) = \frac{\gamma}{2}W^2 + \frac{1}{2}\{\ddot{W}^2 + (W'')^2 + 2\ddot{W}W'' - (1-\mu)[\ddot{W}W'' - (\dot{W}')^2]\} - \frac{N_{\mathrm{cr}}}{2}(\dot{W})^2 \tag{7}$$

The dual variable of the displacement W can be obtained as

$$p_1 = \frac{\delta L}{\delta \dot{W}} = -(\dddot{W} + \dot{W}'') - N_{\mathrm{cr}}\dot{W} \tag{8}$$

Let bending angle ψ_x be regarded as the fundamental variables and introducing $\mathbf{q} = \{W, \psi_x\}^{\mathrm{T}} \equiv \{q_1, q_2\}^{\mathrm{T}}$, the Lagrange function can be rewritten as

$$L(q_1, q_2) = \frac{\gamma}{2}q_1^2 + \frac{1}{2}\{(-\dot{q}_2 + q_1'')^2 - (1-\mu)[\ddot{q}_1 q_1'' - (\dot{q}_1')^2]\} - \frac{N_{\mathrm{cr}}}{2}q_2^2 \tag{9}$$

The Hamiltonian formulation requires the dual vector $\mathbf{p}$ as

$$\mathbf{p} = \begin{Bmatrix} p_1 \\ p_2 \end{Bmatrix} = \frac{\delta L}{\delta \dot{\mathbf{q}}} = \begin{Bmatrix} -(\ddot{q}_1 + \dot{q}_1'') - N_{\mathrm{cr}}q_2 \\ -(-\dot{q}_2 + q_1'') \end{Bmatrix} \tag{10}$$

The physical components of the dual vector $\mathbf{p}$ consists of the dimensionless effective shear and moment, or

$$\begin{cases} p_1 = \dfrac{r^2}{D}(Q_x + N\psi_x) = -\left[\left(\dfrac{\partial^3 W}{\partial X^3} + \dfrac{\partial^3 W}{\partial X \partial \theta^2}\right) + N_{\mathrm{cr}}\dfrac{\partial W}{\partial X}\right] \\ p_2 = \dfrac{r}{D}\dfrac{M_x + M_\theta}{1+\mu} = -\left(\dfrac{\partial^2 W}{\partial X^2} + \dfrac{\partial^2 W}{\partial \theta^2}\right) \end{cases} \tag{11}$$

The mutual dual vectors $\mathbf{q}$and $\mathbf{p}$ are regarded as independent variables. Based on these dual vectors, the Hamiltonian function can be introduced as

$$H(\mathbf{q}, \mathbf{p}) = \mathbf{p}^{\mathrm{T}}\dot{\mathbf{q}} - L(\mathbf{q}, \mathbf{p}) = \frac{1}{2}p_2^2 - p_1 q_2 + p_2 q_1'' - \frac{\gamma}{2}q_1^2 + \frac{1}{2}N_{\mathrm{cr}}q_2^2 \tag{12}$$

Substituting Eq. (12) into the variational equation

$$\delta \int [\mathbf{p}^{\mathrm{T}}\dot{\mathbf{q}} - H(\mathbf{q}, \mathbf{p})]\mathrm{d}\Omega = 0 \tag{13}$$

then the fundamental equations, or the dual equations, of the Hamiltonian system can be obtained via integration by parts as

$$\begin{cases} \dot{\mathbf{q}} = \dfrac{\delta H}{\delta \mathbf{p}} \\ \dot{\mathbf{p}} = -\dfrac{\delta H}{\delta \mathbf{q}} \end{cases} \tag{14}$$

Rewriting Eq. (14) in matrix-vector form, one has

$$\begin{Bmatrix} \dot{q}_1 \\ \dot{q}_2 \\ \dot{p}_1 \\ \dot{p}_2 \end{Bmatrix} = \begin{bmatrix} 0 & -1 & 0 & 0 \\ \partial_\theta^2 & 0 & 0 & 1 \\ \gamma & 0 & 0 & -\partial_\theta^2 \\ 0 & -N_{\mathrm{cr}} & 1 & 0 \end{bmatrix} \begin{Bmatrix} q_1 \\ q_2 \\ p_1 \\ p_2 \end{Bmatrix} \tag{15}$$

It can be proven that Eq. (15) indicate directly equilibrium of forces and moments.

Let the state vector be $\psi = \{\mathbf{q}^{\mathrm{T}}, \mathbf{p}^{\mathrm{T}}\}^{\mathrm{T}}$, Eq. (15) can be rewritten as

$$\dot{\psi} = \mathbf{H}\psi. \tag{16}$$

The solution of Eq. (16) can be represented by

$$\psi(X,\theta) = \sum \psi_m(\theta) \mathrm{e}^{\lambda_m X} \tag{17}$$

where ψ_m and λ_m are unknown eigenfunction and eigenvalue, respectively, of the eigenproblem

$$\mathbf{H}\psi_m = \lambda_m \psi_m \tag{18}$$

It can be proven that (i) $\mathbf{H}$ is Hamiltonian operator matrix; (ii) the Hamiltonian eigenproblem (18) has an adjoint symplectic orthogonality relationship between its eigenvectors; (iii) if λ_m is an eigenvalue, $-\lambda_m$ is also an eigenvalue; (iv) the space of eigenvectors, which is formulated by eigensolutions, is complete; and (v) any state vector ψ can always be expanded by a linear combination of the eigen-function-vectors. The proof can be referred to Zhong (2004) and Xu et al. (1997b).

5. The eigenvalue solutions and the sub-symplectic system

Consider the eigenvalue problem which is separable into zero and non-zero eigenvalue solutions. In particular, zero is one of the eigenvalues, or $\lambda = 0$. In this case Eq. (16) becomes $H\psi = 0$. The solution is evidently a form of the buckling in only the circumferential direction, which is independent of the longitudinal coordinate, and it is not within the scope of this paper. For the problem of non-zero eigenvalue ($\lambda \neq 0$), a sub-symplectic system is introduced. The Lagrange function (7) can be expressed as

$$L(W) = \frac{1}{2}(\gamma + \lambda^4 - N_{\mathrm{cr}}\lambda^2)W^2 + \frac{1}{2}\{(W'')^2 + 2\lambda^2 WW'' - (1-\mu)\lambda^2[WW'' - (W')^2]\} \tag{19}$$

where coordinate θ is taken in analogy to the time coordinate. Introducing $\mathbf{f} = \{W, \phi\}^{\mathrm{T}} \equiv \{f_1, f_2\}^{\mathrm{T}}$ where $\phi = -W'$ and similar to Eqs. (8)–(10), the dual variables are obtained as

$$\mathbf{g} = \begin{Bmatrix} g_1 \\ g_2 \end{Bmatrix} = \frac{\delta L}{\delta \mathbf{f}'} = \begin{Bmatrix} -(f_1''' + \lambda^2 f_1') \\ -(-f_2'' + \lambda^2 f_1) \end{Bmatrix} \tag{20}$$

The dual vector $\mathbf{g}$ denotes shear and moment. The other Hamiltonian function is

$$H(\mathbf{f},\mathbf{g}) = \mathbf{g}^{\mathrm{T}}\mathbf{f}' - L(\mathbf{f},\mathbf{g}) = \frac{1}{2}g_2^2 - g_1 f_2 + \lambda^2 g_2 f_1 - \frac{1}{2}(\gamma - N_{\mathrm{cr}}\lambda^2)f_1^2 \tag{21}$$

The Hamiltonian dual equations can be written as

$$\begin{Bmatrix} f_1' \\ f_2' \\ g_1' \\ g_2' \end{Bmatrix} = \begin{bmatrix} 0 & -1 & 0 & 0 \\ \lambda^2 & 0 & 0 & 1 \\ \gamma - \lambda^2 N_{\mathrm{cr}} & 0 & 0 & -\lambda^2 \\ 0 & 0 & 1 & 0 \end{bmatrix} \begin{Bmatrix} f_1 \\ f_2 \\ g_1 \\ g_2 \end{Bmatrix} \tag{22}$$

or

$$\varphi' = \mathbf{H}_s \varphi \tag{23}$$

where $\varphi = \{\mathbf{f}^{\mathrm{T}}, \mathbf{g}^{\mathrm{T}}\}^{\mathrm{T}}$ is the state vector. In the symplectic space, the solution can be represented by

$$\varphi(\theta) = \sum A_n \mathbf{e}^{\eta_n \theta} \tag{24}$$

and the eigensolutions constitute a complete space of solutions where η_n is the eigenvalue and A_n is a constant vector. It is noticed that the boundary conditions of solution (24) are given on $\theta = 0$ and $\theta = 2\pi$ since the cylindrical shell is a closed shell. The boundary conditions and the continuous conditions are expressed as

$$f_1|_{\theta=0} = f_1|_{\theta=2\pi}, \quad f_2|_{\theta=0} = f_2|_{\theta=2\pi}, \quad g_1|_{\theta=0} = g_1|_{\theta=2\pi}, \quad g_2|_{\theta=0} = g_2|_{\theta=2\pi} \tag{25}$$

or

$$\varphi(0) = \varphi(2\pi) \tag{26}$$

In other words, the eigenvalue must satisfy the equation $\eta_n = ni$ ($n = 0, \pm 1, \pm 2, \ldots$). In sub-symplectic system, the zero eigenvalue solutions and the non-zero eigenvalue solutions have an important physical meaning. The zero eigenvalue solutions ($n = 0$) are related to axisymmetric buckling modes whereas the non-zero eigenvalue solutions ($n \neq 0$) denote non-axisymmetric buckling.

It can be easily verified that solutions (17) and the function in solution (24) are related by

$$\psi(X,\theta) = \sum_m \sum_n B_{mn} e^{\lambda_m X} e^{in\theta} \equiv \sum_n \bar{\psi}(N_{cr}, n, X) e^{in\theta} \tag{27}$$

where B_{mn} is a constant vector and λ is the load function N_{cr}. The critical load N_{cr} can be very large which corresponds to λ_m having a large m, namely $\lambda = \lambda_m$ ($m = 0, 1, 2, \ldots$). Substituting solution (27) into Eq. (15) yields a characteristic polynomial as follows:

$$\begin{vmatrix} -\lambda & -1 & 0 & 0 \\ -n^2 & -\lambda & 0 & 1 \\ \gamma & 0 & -\lambda & n^2 \\ 0 & -N_{cr} & 1 & -\lambda \end{vmatrix} = 0 \tag{28}$$

or

$$\lambda^4 + (N_{cr} - 2n^2)\lambda^2 + \gamma + n^4 = 0 \tag{29}$$

where the components of the constant vector are expressed as

$$B_{mn}^{(1)} = b_{mn}, \quad B_{mn}^{(2)} = -\lambda b_{mn}, \quad B_{mn}^{(3)} = [(\lambda n^2 - \lambda^3) + N_{cr}\lambda] b_{mn}, \quad B_{mn}^{(4)} = (n^2 - \lambda^2) b_{mn} \tag{30}$$

Since there are four roots for eigenequation (29), the general eigensolution should be

$$\begin{cases} \bar{q}_1 = b_{1n}\cos(\alpha_1 X) + b_{2n}\sin(\alpha_1 X) + b_{3n}\cos(\alpha_2 X) + b_{4n}\sin(\alpha_2 X) \\ \bar{q}_2 = b_{1n}\alpha_1\sin(\alpha_1 X) - b_{2n}\alpha_1\cos(\alpha_1 X) + b_{3n}\alpha_2\sin(\alpha_2 X) - b_{4n}\alpha_2\cos(\alpha_2 X) \\ \bar{p}_1 = b_{1n}[\alpha_1(n^2 + N_{cr}) - \alpha_1^3]\sin(\alpha_1 X) - b_{2n}[\alpha_1(n^2 + N_{cr}) - \alpha_1^3]\cos(\alpha_1 X) \\ \qquad + b_{3n}[\alpha_2(n^2 + N_{cr}) - \alpha_2^3]\sin(\alpha_2 X) - b_{4n}[\alpha_2(n^2 + N_{cr}) - \alpha_2^3]\cos(\alpha_2 X) \\ \bar{p}_2 = b_{1n}(\alpha_1^2 + n^2)\cos(\alpha_1 X) + b_{2n}(\alpha_1^2 + n^2)\sin(\alpha_1 X) \\ \qquad + b_{3n}(\alpha_2^2 + n^2)\cos(\alpha_2 X) + b_{4n}(\alpha_2^2 + n^2)\sin(\alpha_2 X) \end{cases} \tag{31}$$

where

$$\begin{cases} \alpha_1 = \left\{ \frac{N_{cr}}{2} - n^2 + \left[\left(\frac{N_{cr}}{2}\right)^2 - n^2 N_{cr} - \gamma \right]^{1/2} \right\}^{1/2} \\ \alpha_2 = \left\{ \frac{N_{cr}}{2} - n^2 - \left[\left(\frac{N_{cr}}{2}\right)^2 - n^2 N_{cr} - \gamma \right]^{1/2} \right\}^{1/2} \end{cases} \tag{32}$$

The solution (31) can be represented by

$$\bar{\psi}(N_{\mathrm{cr}}, n, X) = \mathbf{A}(N_{\mathrm{cr}}, n, X)\mathbf{b} \tag{33}$$

where the undetermined vector is $\mathbf{b} = \{b_{1n}, b_{2n}, b_{3n}, b_{4n}\}^{\mathrm{T}}$. The solution (31) or (33) implies one restriction, i.e. each and every wave length of the buckling mode along the centroidal axis is limited. To explain the phenomena, we suppose the wave front is $X_{\mathrm{e}} = T$ (or $x_{\mathrm{e}} = ct$), $N_{\mathrm{cr}}/2 - n^2 > [n^4 + \gamma]^{1/2}$. The wave length has m-order and it depicts wrinkling of the buckling mode along the centroidal axis. Therefore, $\alpha_1 T \leqslant 2m\pi$ and $\alpha_2 T \leqslant 2m\pi$. The result is $\alpha_1\alpha_2 T^2 \leqslant 4m^2\pi^2$, namely

$$T \leqslant \frac{\sqrt{2}m\pi}{[\gamma + n^4]^{1/4}} \quad \text{or} \quad t \leqslant \frac{\sqrt{2}m\pi r}{c[\gamma + n^4]^{1/4}} \tag{34}$$

In other words, the order of buckling mode can only be less than m-order, and it is not dependent on the load but rather dependent on the parameters of material and structure.

6. The continuous conditions of end boundary and wave front

The end boundary conditions of the shell can be derived from Eq. (13). Suppose $X = X_0$ be any end of the shell, we have

$$\begin{cases} q_1 = 0 \quad \text{or} \quad p_1 = 0 & (X = X_0) \\ q_2 = 0 \quad \text{or} \quad p_2 - (1-\mu)\partial_\theta^2 q_1 = 0 & (X = X_0) \end{cases} \tag{35}$$

The typical end conditions are fixed, simple supports and free supports. These conditions can be expressed, respectively, as

$$q_1 = 0; \quad q_2 = 0 \qquad (X = X_0) \tag{36}$$

$$q_1 = 0; \quad p_2 - (1-\mu)\partial_\theta^2 q_1 = 0 \qquad (X = X_0) \tag{37}$$

$$p_1 = 0; \quad p_2 - (1-\mu)\partial_\theta^2 q_1 = 0 \qquad (X = X_0) \tag{38}$$

The equipollent boundary conditions of ends of the shell in Eqs. (36)–(38) can be rewritten as, respectively,

$$\bar{q}_1 = 0; \quad \bar{q}_2 = 0 \qquad (X = X_0) \tag{39}$$

$$\bar{q}_1 = 0; \quad \bar{p}_2 = 0 \qquad (X = X_0) \tag{40}$$

$$\bar{p}_1 = 0; \quad \bar{p}_2 + (1-\mu)n^2\bar{q}_1 = 0 \qquad (X = X_0) \tag{41}$$

If the wave does not reflect, the region $T < X \leqslant L$ ($ct < x \leqslant l$) is non-disturbed and the internal force and displacement are equal to zero. Therefore the continuous conditions of the wave front should be

$$\bar{q}_1 = 0; \quad \bar{q}_2 = 0 \qquad (X = T) \tag{42}$$

Otherwise, the shell is divided into two regions after the wave has reflected. From Eq. (6), the axial internal forces are different in both regions and the displacements can be non-zero. In this case, two solutions exist in the two regions and they should satisfy the continuous conditions on the wave front of reflection ($X = X_r$). Let solutions (27) be, respectively, $\psi^{(1)}(N_{\mathrm{cr}}, X, \theta)$ and $\psi^{(2)}(N^*_{\mathrm{cr}}, X, \theta)$, or $\bar{\psi}^{(1)}(N_{\mathrm{cr}}, n, X)$ and $\bar{\psi}^{(2)}(N^*_{\mathrm{cr}}, k, X)$. Owing to the continuous conditions at $X = X_r$ along coordinate θ, the result obtained is such that k must be equal to n from solutions (27). The continuous conditions about coordinate X can be reduced to

$$\bar{q}_1^{(1)} = \bar{q}_1^{(2)}; \quad \bar{q}_2^{(1)} = \bar{q}_2^{(2)}; \quad \bar{p}_1^{(1)} = \bar{p}_1^{(2)}; \quad \bar{p}_2^{(1)} = \bar{p}_2^{(2)} \qquad (X = X_r) \tag{43}$$

or

$$\bar{\psi}^{(1)}(N_{\mathrm{cr}}, n, X_r) = \bar{\psi}^{(2)}(N^*_{\mathrm{cr}}, n, X_r) \tag{44}$$

Eqs. (43) or (44) indicate continuous displacements, bending angles, effective shears and moments, respectively.

7. The bifurcated condition of buckling

In this section, the bifurcated conditions of buckling are discussed in two parts, i.e. reflection of wave and non-reflection of wave. The case of fixed end supports with wave reflection is discussed in detail.

First, we investigate the case with stress wave propagating along the shell. A step load impacts one end of the shell at the moment when the propagating wave has not reached the other end. In this case, the solution (31) or (33) should satisfy boundary conditions (39) and continuous conditions of the wave front (42). The linear homogeneous equations for the undetermined constants are obtained as

$$\begin{bmatrix} A_{k1}(N,n,0) & A_{k2}(N,n,0) & A_{k3}(N,n,0) & A_{k4}(N,n,0) \\ A_{j1}(N,n,0) & A_{j2}(N,n,0) & A_{j3}(N,n,0) & A_{j4}(N,n,0) \\ A_{11}(N,n,X_e) & A_{12}(N,n,X_e) & A_{13}(N,n,X_e) & A_{14}(N,n,X_e) \\ A_{21}(N,n,X_e) & A_{22}(N,n,X_e) & A_{23}(N,n,X_e) & A_{24}(N,n,X_e) \end{bmatrix} \mathbf{b} = 0 \tag{45}$$

where $A_{5k}(N_{\mathrm{cr}}, n, X) \equiv A_{4k}(N_{\mathrm{cr}}, n, X) + (1-\mu)n^2 A_{1k}(N_{\mathrm{cr}}, n, X)$ $(k = 1, 2, 3, 4)$. In Eq. (45), $k = 1$, $j = 2$; $k = 1$, $j = 3$ and $k = 3$, $j = 5$ represent the cases of fixed, simple supports and free supports on the impact end, respectively.

Next, we investigate the case after the wave has reflected from the other end of the shell. In this case, the shell is partitioned into two regions. Let $\bar{\psi}^{(1)}(N_{\mathrm{cr}}, n, X) \equiv \mathbf{A}^{(1)}(X)\mathbf{b}^{(1)}$ and $\bar{\psi}^{(2)}(2N_{\mathrm{cr}}, n, X) \equiv \mathbf{A}^{(2)}(X)\mathbf{b}^{(2)}$ be solutions in the two regions, respectively. The former satisfy one boundary condition (39) at $X_0 = 0$ and the latter satisfy the other boundary condition (39) at $X_0 = L$. Both of them satisfy the continuous conditions (44) at $X = X_r$. The equations can be combined into

$$\begin{bmatrix} A^{(1)}_{k1}(0) & A^{(1)}_{k2}(0) & A^{(1)}_{k3}(0) & A^{(1)}_{k4}(0) & 0 & 0 & 0 & 0 \\ A^{(1)}_{j1}(0) & A^{(1)}_{j2}(0) & A^{(1)}_{j3}(0) & A^{(1)}_{j4}(0) & 0 & 0 & 0 & 0 \\ A^{(1)}_{11}(X_r) & A^{(1)}_{12}(X_r) & A^{(1)}_{13}(X_r) & A^{(1)}_{14}(X_r) & A^{(2)}_{11}(X_r) & A^{(2)}_{12}(X_r) & A^{(2)}_{13}(X_r) & A^{(2)}_{14}(X_r) \\ A^{(1)}_{21}(X_r) & A^{(1)}_{22}(X_r) & A^{(1)}_{23}(X_r) & A^{(1)}_{24}(X_r) & A^{(2)}_{21}(X_r) & A^{(2)}_{22}(X_r) & A^{(2)}_{23}(X_r) & A^{(2)}_{24}(X_r) \\ A^{(1)}_{31}(X_r) & A^{(1)}_{32}(X_r) & A^{(1)}_{33}(X_r) & A^{(1)}_{34}(X_r) & A^{(2)}_{31}(X_r) & A^{(2)}_{32}(X_r) & A^{(2)}_{33}(X_r) & A^{(2)}_{34}(X_r) \\ A^{(1)}_{41}(X_r) & A^{(1)}_{42}(X_r) & A^{(1)}_{43}(X_r) & A^{(1)}_{44}(X_r) & A^{(2)}_{41}(X_r) & A^{(2)}_{42}(X_r) & A^{(2)}_{43}(X_r) & A^{(2)}_{44}(X_r) \\ 0 & 0 & 0 & 0 & A^{(2)}_{11}(L) & A^{(2)}_{12}(L) & A^{(2)}_{13}(L) & A^{(2)}_{14}(L) \\ 0 & 0 & 0 & 0 & A^{(2)}_{21}(L) & A^{(2)}_{22}(L) & A^{(2)}_{23}(L) & A^{(2)}_{24}(L) \end{bmatrix} \begin{Bmatrix} \mathbf{b}^{(1)} \\ \mathbf{b}^{(2)} \end{Bmatrix} = 0 \tag{46}$$

Let Eq. (45) and Eq. (46) be rewritten uniformly as

$$\mathbf{B}\mathbf{b} = 0 \tag{47}$$

If the solution (31) or (33) is zero at all time, buckling of the shell does not occur. Otherwise, the condition that Eq. (31) has non-zero solution is transformed into Eq. (47), i.e., at the bifurcation point, the determinant of the coefficient matrix is zero, or

$$|\mathbf{B}| = 0. \tag{48}$$

From the bifurcation condition (48), the critical buckling load N_{cr} can be determined. Furthermore, the corresponding mode of buckling at a specific time can be solved from Eqs. (47), (31) and (27). It should be pointed that buckling modes are complex expressions. Both real and imaginary parts of the expressions are solutions of the problem. The discrepancy between them can be represented by an angle phase shift.

8. Numerical results of critical buckling load and modes of the buckling

For simplicity, let $R = 1$, $L = 5$, $h/r = 0.05$, $X_e = T$ and the critical buckling load $N_{cr} = Nr^2/D$. Eqs. (36) or (39) are considered as the ends boundary condition and others are similar. When the end of shell is subjected to a step impact load, the longitudinal wave starts to propagate with wave speed c determined by the material and structure. Furthermore, let $X_e = T$ be the position of propagation of wave.

When buckling of shell occurs at a specific time, the critical buckling loads N_{cr} can be determined by the bifurcation condition (48). At that time, the impact load N_{cr} causes the shell to buckle. Figs. 1–3 illustrate curves of critical buckling load with wave propagation time. In these figures, it can be observed that the critical loads decrease with time. Moreover, $X_e = 5$ is a point that the wave reflects and the critical buckling loads decrease obviously after the reflection of wave. Let n be defined as the order in Eq. (27) and it shows the stage of non-axisymmetric buckling. In fact, from Eq. (27) n represents the number of corrugations for circumferential buckling. For a fixed n, the critical load has multi-branches which are marked as the first branch with $m = 1$, the second branch with $m = 2$, and the like. The branch indicates the number of corrugations for axial buckling. Fig. 1 shows the first 10 orders of critical load curves. The buckling load increases with increasing n. The critical loads of axisymmetric buckling ($n = 0$) and non-axisymmetric buckling ($n = 2$) are displayed for the first 10 branches of critical load curves in Figs. 2 and 3, respectively. For each branch, the critical load is greater for higher order modes. This phenomenon shows that non-axisymmetric critical load is higher than axisymmetric one and this phenomenon is in agreement with

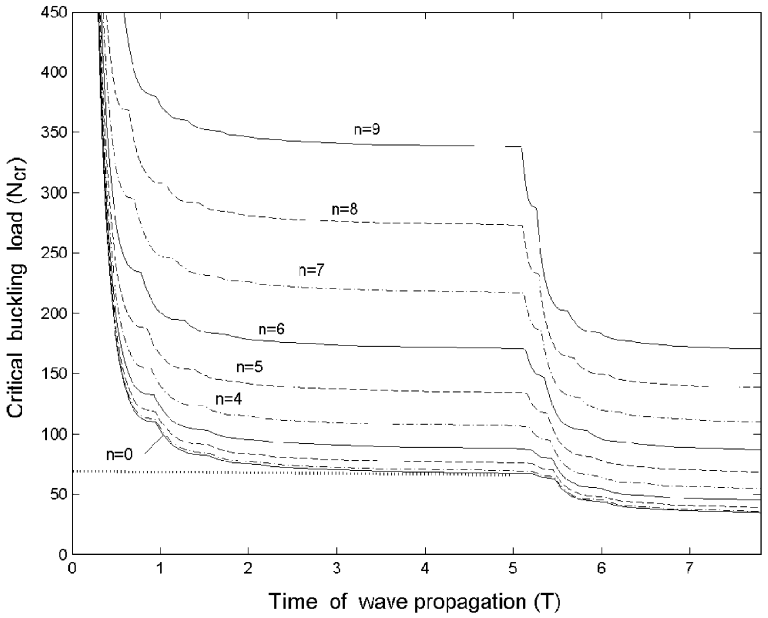

Fig. 1. The first 10 orders of critical buckling loads with time of wave propagation.

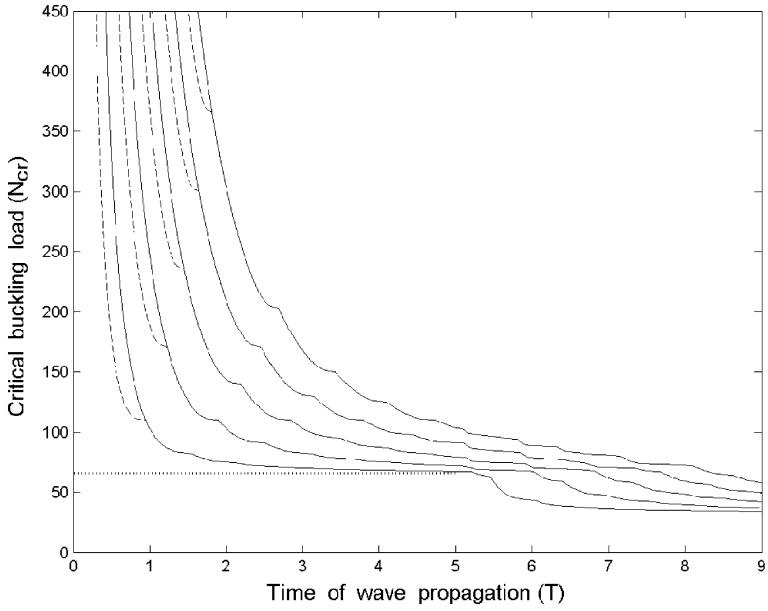

Fig. 2. The first 10 branches of critical buckling loads with time of wave propagation ($n = 0$).

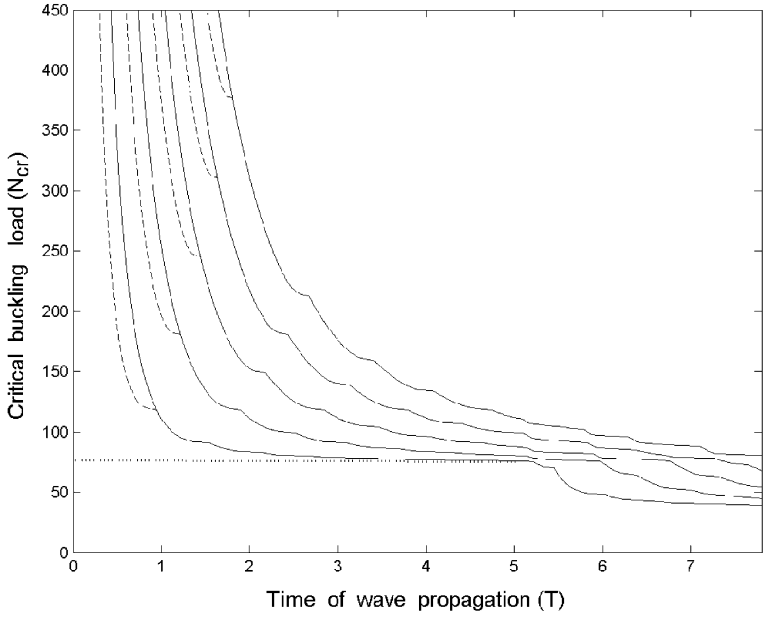

Fig. 3. The first 10 branches of critical buckling loads ($n = 2$).

experiments in the middle thickness shell that is impacted by the axial load (Wang et al., 1983; Chen et al., 1992). This fact implies axisymmetric buckling occurs more easily as compared to non-axisymmetric buckling. It is noteworthy that the curves of critical loads of odd branches (dashed lines) coalesces with one-level-higher even branches (continuous lines) as observed in Figs. 2 and 3. The phenomenon explains that

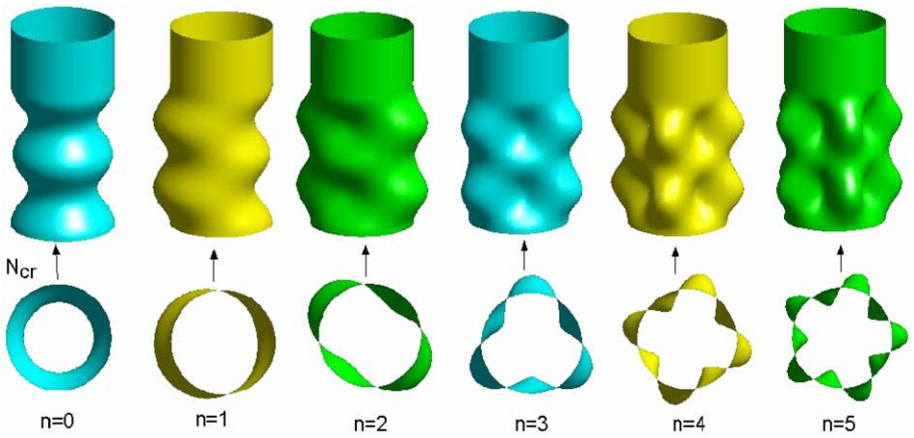

Fig. 4. Six circumferential buckling modes ($n = 0, 1, 2, 3, 4, 5$; $X_e = T = 3.5$).

half wave length of buckling mode occurs in even multiples only and buckling takes place in a short time. Besides, dot lines, in Figs. 1–3, are stated critical load. It shows that the stated critical loads are lower than dynamic ones before wave reflection. After wave reflection ($T > 5$ in figures), the axial force in shell is $2N$ but N in the reflection region so as to some dynamic critical loads can be lower than the stated critical load since the axial impact load is step one. If the wave reflects to the impacted end, the axial force in whole shell is $2N$ and it can be imagined that the stated critical load reduces to half of it. In this case, the dynamic buckling is the easier than stated one. The numerical result shows that the dynamic critical load is the greater than half of the stated critical load before second reflection of the wave on the impacted end.

After solving the critical buckling load N_{cr} by bifurcation condition (48), the corresponding buckling mode can be obtained from Eqs. (47), (31) and (27). Assuming the top of shell is the wave reflection end while the other end is subjected to an impact load, Fig. 4 shows six buckling modes ($n = 0, 1, 2, 3, 4, 5$; $X_e = T = 3.5$) with critical loads corresponding to Fig. 1. The order of circumferential buckling is given by n where $n = 0$ represents axisymmetric buckling and $n \neq 0$ denotes non-axisymmetric modes. The level of complexity of non-axisymmetry increases with increasing n.

It is also noticed from Figs. 1–3 that there exist many inflexions for the critical load curves. In reality, the inflexions interrelate with the limit (34) of wrinkle of buckling mode along the centroidal axis. Fig. 5 shows this character (the lowest branch curve in Fig. 3 is selected as the critical load and critical time $T = 0.5, 0.8, 1.2, 1.8, 3.0, 4.5$, respectively) where the buckling modes for loads between two inflexions on one curve, or there are multi-branches on one curve of critical load.

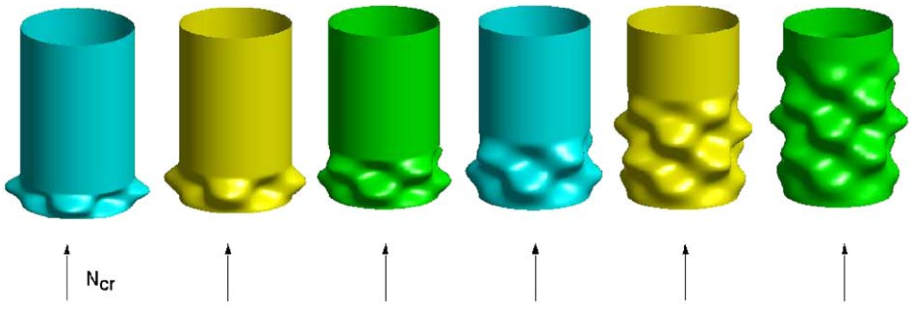

Fig. 5. Multi-branches of buckling modes.

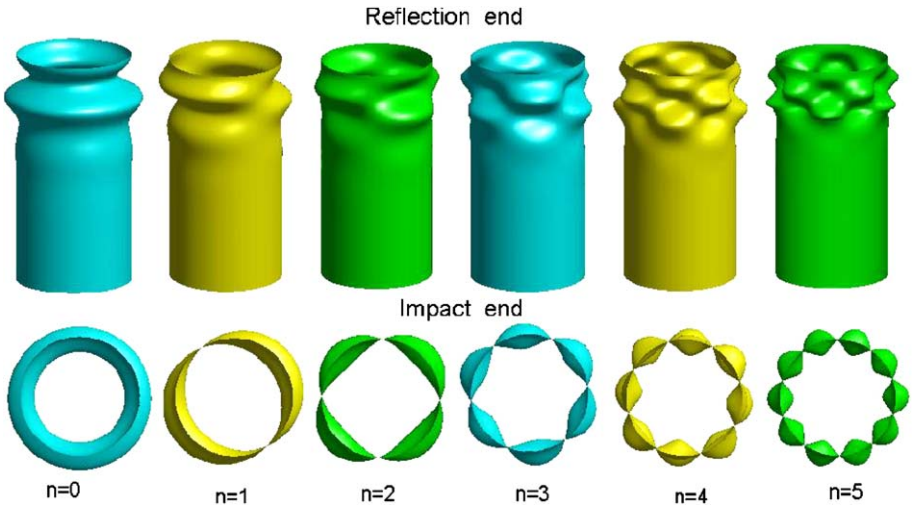

Fig. 6. Buckling modes after reflection of wave ($n = 0, 1, 2, 3, 4, 5$; $T = 6$).

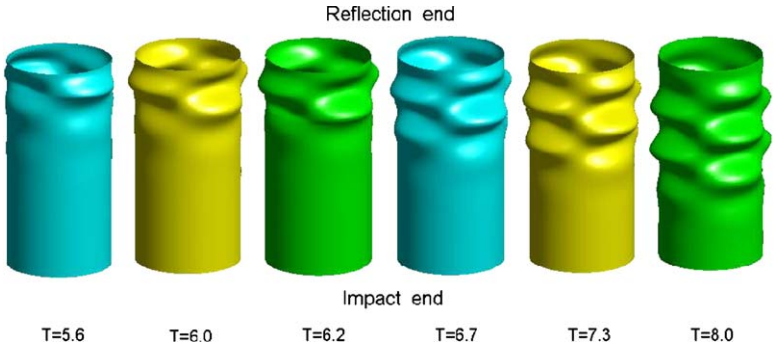

Fig. 7. Various buckling modes with time of reflection.

Because wave reflects from the impact end to the reflection end, the buckling modes of shell have special forms. The buckling modes after reflection of wave are shown in Figs. 6 and 7. Fig. 6 presents six buckling modes ($n = 0, 1, 2, 3, 4, 5$; $T = 6$) with critical loads correspond to Fig. 1. In this figure, it is evident that buckling shapes are extrusive round the reflection end of the shell. Corresponding to the critical loads in Fig. 3, Fig. 7 displays various buckling modes of reflection with time ($n = 2$; $T = 5.6, 6.0, 6.7, 7.3, 8.0$, respectively) where the leftmost mode in the figure refers to the particular moment the wave just arrives at the reflection end. Buckling at the reflection end takes place easily as illustrated in Figs. 6 and 7. This phenomenon agrees with experiments where buckling may occur first at the impact end for high impact load, or otherwise buckling may occur at the reflection end.

9. Conclusion

It has been demonstrated that dynamic buckling of finite cylindrical shells is a local phenomenon at some positions in the first instance and it extends in correlation with propagation and reflection of waves. The

primary factors influencing buckling are the impact loads and the boundary condition. The boundary condition is not only an expression of displacements but it forms a problem of mixed boundary conditions involving geometric and natural conditions. An effective Hamiltonian system has been introduced to the dynamic buckling of structures without Lagrange formulation. A symplectic space has also been introduced where the primary and canonical variables incidentally describe the mixed problem. Employing a sub-symplectic system, the non-axisymmetric problem can be precisely reduced to a problem of eigenvalues and eigensolutions where the eigenvalues denote the critical buckling loads and eigensolutions denote the buckling modes. Significant physical implications of dynamic buckling of shells have been illustrated and discussed.

Acknowledgment

The support of National Natural Science Foundation of China (No. 19902014; No. 10272024) is gratefully acknowledged.

References

Abdullah, S., Zeki et al., 2003. The dynamic buckling of an orthotropic cylindrical thin shell under torsion varying as a power function of time. Acta Mechanica Solida Sinica 16 (1), 81–87.

Arbocz, J., Hol, J.M.A.M., 1991. Collapse of axially compressed cylindrical shells with random imperfections. AIAA Journal 29, 2247–2256.

Boutyour, E.H., Zahrouni, H. et al., 2004. Asymptotic-numerical method for buckling analysis of shell structures with large rotations. Journal of Computational and Applied Mathematics 168 (1–2), 77–85.

Chen, C.A., Su, X.Y. et al., 1992. An experimental investigation on the relation between the elastic–plastic dynamic buckling and the stress wave in cylindrical shells subjected to axial impact. In: Proceedings of the International Symposium Intense Dynamic Loading and Its Effects. Chengdu, China, pp. 543–546.

Choong, K.K., Ramm, E., 1998. Simulation of buckling process of shells by using the finite element method. Thin-Walled Structures 31 (1–3), 39–72.

Coppa, A.P., 1960. On the mechanism of buckling of a circular cylindrical shell under longitudinal impact. General Electric Report R60SD494, Presented at Tenth International Congress of Applied Mechanics, Stresa, Italy.

Fettahli, O.A., Steele, C.R., 1974. Asymptotic solutions for orthotropic nonhomogeneous shells of revolution. Journal of Applied Mechanics—Transactions of the ASME 41 (3), 753–758.

Florence, A., Goodier, J.N., 1968. Dynamic plastic buckling of cylindrical shells in sustained axial compressive flow. Journal of Applied Mechanics 35, 80–86.

Hambly, E.T., Calladine, C.R., 1996. Buckling experiments on damaged cylindrical shells. International Journal of Solids and Structures 33 (24), 3539–3548.

Jamal, M., Midani, M. et al., 1999. Influence of localized imperfections on the buckling of cylindrical shells under axial compression. International Journal of Solids and Structures 36 (3), 441–464.

Jamal, M., Lahlou, L. et al., 2004. A semi-analytical buckling analysis of imperfect cylindrical shells under axial compression. International Journal of Solids and Structures 40 (5), 1311–1327.

Karagiozova, D., Alves, M., 2004a. Transition from progressive buckling to global bending of circular shells under axial impact—Part I: Experimental and numerical observations. International Journal of Solids and Structures 41 (5–6), 1565–1580.

Karagiozova, D., Alves, M., 2004b. Transition from progressive buckling to global bending of circular shells under axial impact—Part II: Theoretical analysis. International Journal of Solids and Structures 41 (5–6), 1581–1604.

Karagiozova, D., Jones, N., 2001. Influence of stress waves on the dynamic progressive and dynamic plastic buckling of cylindrical shells. International Journal of Solids and Structures 38 (38–39), 6723–6749.

Karagiozova, D., Jones, N., 2002. On dynamic buckling phenomena in axially loaded elastic–plastic cylindrical shells. International Journal of Non-Linear Mechanics 37 (7), 1223–1238.

Lancaster, E.R., Calladine, C.R., Palmer, S.C., 2000. Paradoxical buckling behaviour of a thin cylindrical shell under axial compression. International Journal of Mechanical Sciences 42 (5), 843–865.

Lim, C.W., Ma, Y.F., 2003. Computational p-element method on the effects of thickness and length on self-weight buckling of thin cylindrical shells via various shell theories. Computational Mechanics 31 (5), 400–408.

Lim, C.W., Ma, Y.F., Kitipornchai, S., Wang, C.M., Yuen, R.K.K., 2003. Buckling of vertical cylindrical shells under combined end pressure and body force. Journal of Engineering Mechanics—Transactions of the ASCE 129 (8), 876–884.

Ma, H.W., Zhang, L.J. et al., 2003. Experimental investigation of the second critical velocity of dynamic buckling of a cylindrical shell under axial impact. Engineering Plasticity from Macroscale to Nanoscale PTS 1 and 2 233-2, 235–238.

Sofiyev, A.H., Aksogan, O., 2004. Buckling of a conical thin shell with variable thickness under a dynamic loading. Journal of Sound and Vibration 270 (4–5), 903–915.

Steele, C.R., Kim, Y.Y., 1992. Modified mixed variational principle and the state-vector equation for elastic bodies and shells of revolution. Journal of Applied Mechanics—Transactions of the ASME 59 (3), 587–595.

Tian, J., Wang, C.M., Swaddiwudhipong, S., 1999. Elastic buckling analysis of ring-stiffened cylindrical shells under general pressure loading via the Ritz method. Thin-Walled Structures 35 (1), 1–24.

Tovstik, P.E., Smirnov, A.L., 2001. Asymptotic Method in the Buckling Theory of Elastic Shells. World Scientific Publishing Co. Pte. Ltd.

Uchiyama, M., Yamada, S., 2003. Nonlinear buckling simulations of imperfect shell domes by mixed finite elements. Journal of Engineering Mechanics—ASCE 129 (7), 707–714.

Wang, R., Han, M.B. et al., 1983. An experimental study on the dynamic axial plastic buckling of cylindrical shells. International Journal of Impact Engineering 1 (3), 249–256.

Xu, X.S., Su, X.Y., Wang, R., 1995. Dynamic buckling of elastic–plastic cylindrical shells on axial stress waves. Science in China (Ser. A) 38 (4), 472–479.

Xu, X.S., Xu, J.Y. et al., 1997a. Dynamic axisymmetric and non-axisymmetric buckling of finite cylindrical shells in propagating and reflecting of axial stress waves. Journal Physique iv France 7 (C3), 617–622.

Xu, X.S., Zhong, W.X., Zhang, H.W., 1997b. The Saint-Venant problem and principle in elasticity. International Journal of Solids and Structures 34 (22), 2815–2827.

Zhong, W.X., 2004. Duality System in Applied Mechanics and Optimal Control. Kluwer Academic Publishers.